CHIN. PHYS. LETT. Vol. 33, No. 2 (2016) 026201

The Mechanism of Critical Strain of Serrated Yielding in Strain Rate Domain *

Shi-Hua Fu(符师桦), Yu-Long Cai(蔡玉龙), Su-Li Yang(杨素丽),
Qing-Chuan Zhang(张青川)**, Xiao-Ping Wu(伍小平)

CAS Key Laboratory of Mechanical Behavior and Design of Materials, Department of Modern Mechanics, University of Science and Technology of China, Hefei 230027

(Received 15 September 2015)

The mechanism of the critical strain of serrated yielding is studied via tension tests at various strain rates. Before the critical strain, it is deduced that dislocations are not pinned at high strain rates, and dislocations at low strain rates are pinned but cannot escape. The critical strain depends on the first pinning process at high strain rates and on the first unpinning process at low strain rates. The calculated results based on the two criteria are in good consistency with the experiment.

PACS: 62.20.F−, 81.05.Bx, 81.40.Cd DOI: 10.1088/0256-307X/33/2/026201

Serrated yielding, called the Portevin–Le Chatelier (PLC) effect, has been observed in many alloys under certain conditions associated with the fluctuant stress–strain curve and localized deformation.[1−4] This phenomenon is explained as dynamic strain aging (DSA),[5−7] i.e., the interaction between mobile dislocations and solute atoms. During the waiting time of mobile dislocations, the solute atoms diffuse to and pin them, elevating additionally the stress level. With the aid of applied stress, the pinned dislocations break away from the solute atoms, leading to a drop in stress level.

The onset of serrated yielding, called the critical strain, has been widely studied. According to the variations of critical strain with strain rate or temperature, two kinds of the critical behaviors are defined.[8] One is the normal behavior that the critical strain increases with increasing the strain rate or decreasing the temperature. The other is the inverse behavior that the critical strain increases with decreasing the strain rate or increasing the temperature.

McCormick[9] proposed a vacancy-assisted model for the critical strain based on the strain-dependent diffusivity of solute atoms and the strain-dependent waiting time. This model works for normal behavior but fails for inverse behavior.

Kubin *et al.*[8] proposed a model with a condition of strain-rate sensitivity equals zero based on the evolution of mobile and forest dislocations. Hähner[10] proposed a model to quantitatively analyze the critical conditions based on additional activation enthalpy owing to DSA. Cai *et al.*[11] proposed a model to reproduce the critical strain. Mazière *et al.*[12] proposed a finite element model with exponential growth criterion to simulate the critical strain in the strain rate domain. However, these models focused on the mathematical model rather than the physical mechanism. Some researchers presented that nitrogen addition elevates the critical strain in an FeMnCN steel[13] and the inverse behavior may be related to stacking faults in a Ni-Co base superalloy,[14] while neither of them involves analyses in the mechanism.

Recently, our group[15] pointed out the distinction of the two critical behaviors on microscopic scale for the first time and proposed two mechanisms for the normal and inverse behaviors of the critical strain in the temperature domain. The critical strain is in relation with the first pinning process at low temperatures and with the first unpinning process at high temperatures. However, in strain rate domain, the two mechanisms have not been verified and it is necessary to reveal the distinction between the physical mechanisms of the normal and inverse critical behaviors. In this work, we investigate the critical behavior at various strain rates in an Al-Mg alloy, improve and extend the mechanisms in Ref. [15] to interpret the critical behavior in the strain rate domain.

The investigated material was a commercial Al-Mg (type 5456) alloy. The chemical composition (wt.%) is Mg 4.7–5.5, Mn 0.5–1.0, Fe 0.4, Si 0.25, Zn 0.25, Ti 0.2, Cu 0.1, Cr 0.05–0.2, balance Al. Before tension, the samples with gauge length, width and thickness of 55, 20 and 3 mm, respectively, were annealed at 673 K for 3 h and then furnace-cooled to room temperature. The tensile tests were carried out at various nominal strain rates ranging from 1.8×10^{-5} to $1.8\times10^{-2}\,\mathrm{s}^{-1}$ with a sampling rate of 100 Hz.

The stress–strain curves at various strain rates are shown in Fig. 1(a). For a better view, the curves are separated by an interval of 50 MPa. The results show that the serrated yielding was absent at the lowest strain rate. The variation of the critical strain with

*Supported by the National Natural Science Foundation of China under Grant Nos 11332010, 51271174 and 51571013, and the Fundamental Research Funds for the Central Universities.

**Corresponding author. Email: zhangqc@ustc.edu.cn

© 2016 Chinese Physical Society and IOP Publishing Ltd

strain rate is shown in Fig. 1(b). The critical strain first decreases and then increases with increasing the strain rate. The descending branch at low strain rates is an inverse behavior while the ascending branch at high strain rate is a normal behavior.

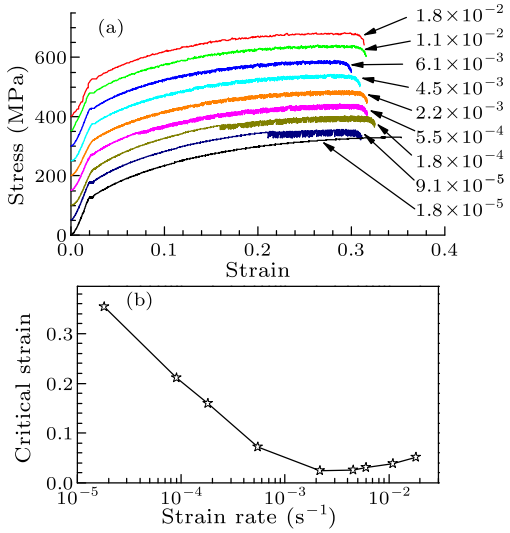

Fig. 1. (a) Stress–strain curves at various strain rates. (b) Variation of the critical strain. For a better view, the stress–strain curves are separated by an interval of 50 MPa. With increasing the strain rate, the critical strain decreases at low strain rates (inverse behavior) and then increases at high strain rates (normal behavior).

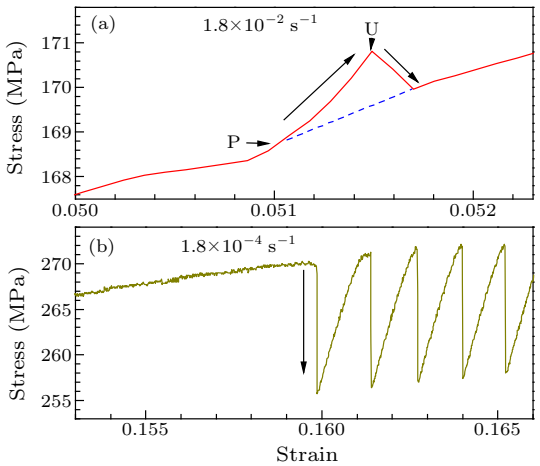

Fig. 2. Different serration directions: (a) upward serration at $1.8 \times 10^{-2}\,s^{-1}$ and (b) downward serration at $1.8 \times 10^{-4}\,s^{-1}$. The blue dashed line is the hypothetical stress in the absence of serration. At $1.8 \times 10^{-2}\,s^{-1}$, the stress is elevated additionally in section PU and the stress drops sharply after point U. At $1.8 \times 10^{-4}\,s^{-1}$, the stress drops sharply from a higher level to a lower level.

The details of the stress–strain curves near the critical strain are shown in Fig. 2. The serrations are upward at high strain rates while downward at low strain rates. At high strain rates, when serration appears for the first time, the stress is elevated additionally in section PU and then drops sharply after point U. It is suggested that dislocations are not pinned before point P, are pinned in section PU, and are breaking away at point U. The critical strain, to be exact, is point U, where the first unpinning process (yielding) occurs. Noting that the strain interval of section PU is very small (≈0.0007), the critical strain can be considered as point P, where the pinning process begins. At low strain rates, when serration appears for the first time, the stress drops sharply from a higher level to a lower level. This implies that dislocations are pinned by solute atoms but cannot escape before the critical strain. The requirement of the unpinning process is satisfied at the critical strain. Therefore, the critical strain is dependent on the first pinning process at high strain rates and on the first unpinning process at low strain rates. The two cases are discussed separately in the following.

At high strain rates, the critical strain is related to where the pinning process takes place. The pinning process requires that the concentration of solute atoms at mobile dislocation C reaches the minimum value required for pinning which is a constant. At critical strain ε_c, we can obtain[15–17]

$$C(\varepsilon_c) \propto cT^{-1/3}D^{1/3}t_w(\varepsilon_c)^{1/3} = \text{const}, \tag{1}$$

where c is the concentration of solute atoms in the matrix, T is the ambient temperature, D is the diffusion coefficient, and t_w is the waiting time of dislocation. In this study, c and T are constant and thus, D is also constant. For the small ε_c at high strain rates, t_w can be expressed as a linear relationship

$$t_w = (\varepsilon - \varepsilon_y)/\dot{\varepsilon}, \tag{2}$$

where ε_y is the yield strain. Substituting Eq. (2) into Eq. (1) yields

$$(\varepsilon_c - \varepsilon_y)/\dot{\varepsilon} = \text{const}. \tag{3}$$

The relationship of the critical strain and strain rate can be expressed as

$$\varepsilon_c = \phi\dot{\varepsilon} + \varepsilon_y, \tag{4}$$

where ϕ is a coefficient. It shows that the critical strain increases linearly with the strain rate.

At low strain rates, the critical strain is dependent on the first unpinning process. The applied stress σ_{app} can be divided into three parts:

$$\sigma_{app} = \sigma_{srs} + \sigma_{unp} + \sigma_{oth}, \tag{5}$$

where σ_{srs} is the stress related to the strain rate sensitivity, σ_{unp} is the stress that contributes for unpinning, and σ_{oth} is the stress required to overcome the other obstacles (such as forest dislocation, precipitation). According to Ref. [18], the stress related to strain rate sensitivity can be expressed as

$$\sigma_{srs}(\dot{\varepsilon}) = S_0 \log(\dot{\varepsilon}/\dot{\varepsilon}_0), \tag{6}$$

where S_0 is the strain rate sensitivity coefficient, and $\dot{\varepsilon}_0$ is the referenced strain rate.

The critical condition for unpinning is that $\sigma_{\rm unp}$ is sufficiently large to overcome the solute obstacles due to DSA,[15] i.e.,

$$\sigma_{\rm unp}(\varepsilon_{\rm c}) = \sigma_{\rm sol}, \tag{7}$$

where $\sigma_{\rm sol}$ is the strength of the solute obstacles due to DSA. The strength of the solute obstacles is reflected by serration amplitude and is proportional to the solute atoms' concentration at mobile dislocation,[17] i.e., $\sigma_{\rm sol} \propto C$. Noting that the serration amplitude is insensitive to strain at high strain rates, according to Eqs. (1) and (2), the relationship of $\sigma_{\rm sol}$ versus $\dot{\varepsilon}$ can be expressed as

$$\sigma_{\rm sol} = \alpha \dot{\varepsilon}^{-1/3}, \tag{8}$$

where α is a coefficient.

At $1.8 \times 10^{-5}\,{\rm s}^{-1}$, the serration yielding is absent, which indicates that dislocations are pinned but cannot escape during the whole deformation process. The stress–strain curve of $1.8 \times 10^{-5}\,{\rm s}^{-1}$ ($\dot{\varepsilon}_1$) can be considered as the upper envelope curve, i.e.,

$$\sigma_{\rm upper} = S_0 \log(\dot{\varepsilon}_1/\dot{\varepsilon}_0) + \sigma_{\rm unp} + \sigma_{\rm oth}. \tag{9}$$

In this study, we do not find a strain rate that is too high to suppress the PLC effect. To estimate the stress in the unpinned state, we remove the serrations from the stress–strain curve of $1.8 \times 10^{-2}\,{\rm s}^{-1}$ ($\dot{\varepsilon}_2$), at which the serration amplitude is smallest. The processed curve is considered as the lower envelope curve, i.e.,

$$\sigma_{\rm lower} = S_0 \log(\dot{\varepsilon}_2/\dot{\varepsilon}_0) + \sigma_{\rm oth}. \tag{10}$$

An illustration for the upper and lower envelope curves is shown in Fig. 3. Subtraction of Eqs. (9) and (10) yields

$$\sigma_{\rm upper} - \sigma_{\rm lower} = \sigma_{\rm unp} - 3S_0. \tag{11}$$

A linear fitting for $\sigma_{\rm upper} - \sigma_{\rm lower}$ is used to simplify the calculation (see the inset of Fig. 3). Therefore, one obtains

$$\sigma_{\rm unp} = \gamma\varepsilon + \beta + 3S_0, \tag{12}$$

where γ and β are determined by fitting.

Substituting Eqs. (8) and (12) into Eq. (7), one obtains

$$\varepsilon_{\rm c} = (\alpha\dot{\varepsilon}^{-1/3} - \beta - 3S_0)/\gamma. \tag{13}$$

As shown in Fig. 4, the calculated curves from Eqs. (4) and (13) are consistent with the experimental data. The left inset shows the linear relationship of $\varepsilon_{\rm c}$ versus $\dot{\varepsilon}^{-1/3}$, and the right inset clearly shows the linear relationship of $\varepsilon_{\rm c}$ versus $\dot{\varepsilon}$. It is suggested that the extended mechanisms are appropriate for explaining the critical behavior in the strain rate domain. At high strain rates, with increasing the strain rate, the waiting time decreases. It is necessary to extend the waiting time for pinning and consequently, the critical strain increases. At low strain rates, the strength of the solute obstacles due to DSA decreases with increasing the strain rate. It is easier to generate the unpinning process and thus the critical strain decreases.

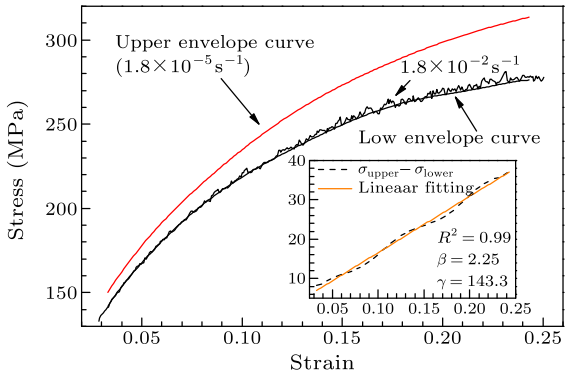

Fig. 3. Illustration for the upper and lower envelope curves. Inset: linear fitting for $\sigma_{\rm upper} - \sigma_{\rm lower}$.

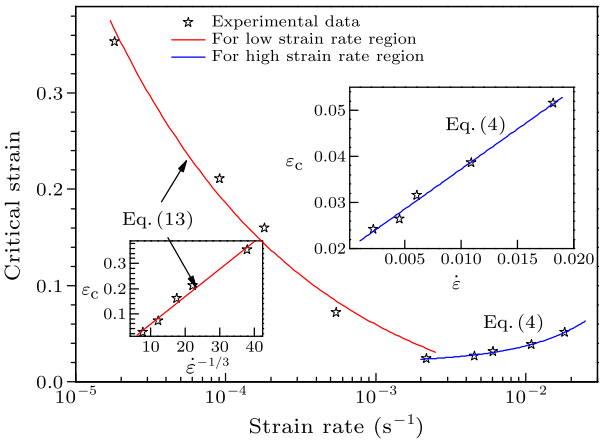

Fig. 4. Comparison between the calculated and experimental results. Left inset: showing the linear relationship of $\varepsilon_{\rm c}$ versus $\dot{\varepsilon}^{-1/3}$; and right inset: showing the linear relationship of $\varepsilon_{\rm c}$ versus $\dot{\varepsilon}$.

In summary, we have investigated the mechanism of the critical strain of serrated yielding in the strain rate domain in 5456 Al-based alloy. At high strain rates, the upward serrations with the normal behavior of critical strain are observed and it suggests that dislocations are not pinned by solute atoms before the critical strain. At low strain rates, the downward serrations with the inverse behavior of critical strain are observed and it suggests that dislocations are pinned by solute atoms but cannot escape before the critical strain. The distinction between the mechanisms of the critical strain for high strain rates and low strain rates is presented. Two criteria are proposed that the critical strain depends on the first pinning process at

high strain rates and on the first unpinning process at low strain rates. The calculated results based on the two criteria are in good consistency with the experiment. These two mechanisms are verified not only in the temperature domain but also in the strain rate domain.

References

[1] Zhao S T, Meng C L, Mao F X, Hu W P and Gottstein G 2014 *Acta Mater.* **76** 54
[2] Fu S H, Gao Y, Cai Y L, Cheng T, Zhang Q C and Wu X P 2015 *Measurement* **72** 61
[3] Choudhary B K 2013 *Mater. Sci. Eng.* A **564** 303
[4] Sun L, Zhang Q C and Cao P T 2009 *Chin. Phys.* B **18** 3500
[5] McCormick P G 1988 *Acta Metall.* **36** 3061
[6] Picu R C 2004 *Acta Mater.* **52** 3447
[7] Curtin W A, Olmsted D L and Hector L G 2006 *Nat. Mater.* **5** 875
[8] Kubin L P and Estrin Y 1990 *Acta Metall. Mater.* **38** 697
[9] McCormick P G 1972 *Acta Metall.* **20** 351
[10] Hähner P 1997 *Acta Mater.* **45** 3695
[11] Cai M C, Niu L S, Yu T, Shi H J and Ma X F 2010 *Mater. Sci. Eng.* A **527** 5175
[12] Mazière M and Dierke H 2012 *Comput. Mater. Sci.* **52** 68
[13] Lee S, Kim J, Lee S J and De Cooman B C 2011 *Scr. Mater.* **65** 528
[14] Cui C Y, Gu Y F, Yuan Y and Harada H 2011 *Scr. Mater.* **64** 502
[15] Fu S H, Cheng T, Zhang Q C, Hu Q and Cao P T 2012 *Acta Mater.* **60** 6650
[16] Springer F, Nortmann A and Schwink C 1998 *Phys. Status Solidi* A **170** 63
[17] Flor H and Neuhäuser H 1980 *Acta Metall.* **28** 939
[18] Hu Q, Zhang Q C, Cao P T and Fu S H 2012 *Acta Mater.* **60** 1647